NASA TN D-1442

TECHNICAL NOTE

D-1442

COMPATIBILITY OF MOLTEN URANIUM DIOXIDE WITH FIVE REFRACTORY MATERIALS

By William A. Sanders and Isadore L. Drell

Lewis Research Center
Cleveland, Ohio

NATIONAL AERONAUTICS AND SPACE ADMINISTRATION
WASHINGTON

January 1963

NATIONAL AERONAUTICS AND SPACE ADMINISTRATION

TECHNICAL NOTE D-1442

COMPATIBILITY OF MOLTEN URANIUM DIOXIDE WITH FIVE REFRACTORY MATERIALS

By William A. Sanders and Isadore L. Drell

SUMMARY

An investigation of the compatibility of molten uranium dioxide with tungsten, tantalum, tantalum diboride, tantalum carbide, and hafnium carbide was conducted to indicate combinations that may be useful in nuclear reactors that are to operate at temperatures above the melting point of uranium dioxide, 5000° F. The evaluations were conducted at a test temperature of 5220° F for a period of 15 minutes in a high-purity argon atmosphere. One compatibility test of molten uranium dioxide with tungsten was conducted at 5500° F. The tests were performed with the refractory material in the form of a crucible that contained a uranium dioxide charge. Crucible cross sections were studied after testing, and the degree of reaction between uranium dioxide and the various crucible materials was judged by the use of X-ray diffraction analysis, metallographic examination, microhardness measurements, and electron-beam microanalysis.

All five materials reacted with molten uranium dioxide at the test temperature of 5220° F. For tungsten, the extent of reaction was slight even at 5500° F. For tantalum, the reaction was greater than but similar in nature to that involving tungsten. For the tantalum diboride and tantalum carbide materials, reactions took place that consumed the entire uranium dioxide charge. For hafnium carbide, a reaction occurred partly because of a boron impurity in the carbide.

INTRODUCTION

New construction materials are needed for the extremely high temperatures obtainable in nuclear-reactor heat sources. These high temperatures are necessary to increase the power output of nuclear reactors proposed for rockets, ramjet and turbojet engines, and electrical powerplants. The refractory metals and refractory compounds have potential for such high-temperature use. The reactor heat source could consist

of uranium dioxide (UO_2) dispersed in a refractory material that provides strength and the required heat-transfer area. For operation above 5000° F, the UO_2 would be in the molten state and should not react with the refractory material if the heat source is to retain its integrity and the reactor is to function properly.

Since thermodynamic and phase-diagram data are insufficient to predict the compatibility of the refractory materials and UO_2 at high temperatures, this research was undertaken. The type of compatibility of concern herein is defined as that state which enables the molten UO_2 and the refractory material to exist in contact with one another without chemical or metallurgical interaction. Low melting or gaseous phases or large volume changes resulting from reactions would be detrimental to reactor operations; however, some reactions in which a new phase is formed may not necessarily preclude the use of a particular material.

The work described herein was undertaken as an extension of a previous investigation (ref. 1) in which the compatibility of UO_2 with 30 refractory metals, carbides, borides, nitrides, and oxides between 3500° and 5000° F was determined. On the basis of the results of that investigation, the more promising materials were selected for the present study.

For this work the following materials were chosen for evaluation with molten UO_2: tungsten (W), tantalum (Ta), tantalum diboride (TaB_2), tantalum carbide (TaC), and hafnium carbide (HfC). The compounds TaB_2 and TaC were included in this study because their degree of reaction with UO_2 up to 5000° F was slight. Although tantalum nitride was reported as being compatible with UO_2 at 5000° F, it was not included in the present study because both the nitride and the UO_2 exhibited very high weight losses at their interfaces at 5000° F.

The five refractory materials were used in the form of high-density crucibles to determine their compatibility with a molten UO_2 charge. Crucible cross sections were studied by various physical means: X-ray diffraction, metallographic examination, microhardness measurements, and electron-beam microanalyses. The electron-beam analyses were performed by the Advanced Metals Research Corporation, Somerville, Massachusetts. A brief description of this method is presented in the appendix.

The compatibility tests were conducted at 5220° F for a period of 15 minutes in a high-purity argon atmosphere. For each material, two

identical runs were made. A new crucible and UO_2 charge were used each time. For tungsten, one test was conducted at 5500° F.

MATERIALS

Chemical, spectrographic, and X-ray diffraction analyses on the UO_2 and crucible materials are given in table I. Also given are the values from the literature for the lattice parameters and the melting points. While the materials were of the highest purity commercially available, it is recognized that higher purity materials might give slightly different results.

Knoop microhardness measurements were made on all the crucibles and on a UO_2 disk. The average values of ten microhardness readings are given in table II. In order that the hardness impressions be confined to a single grain, use of different loads was necessary because of the variance in grain size and hardness of the different materials.

Uranium Dioxide

The UO_2 material used in this investigation was produced in disk form by the supplier with uranium trioxide (UO_3) as the starting material. The disks were 1/2 inch in diameter, 1/4 inch thick, and had 94 percent theoretical density. These disks were fragmented to provide the small pieces needed for the crucible charges.

Crucibles

The crucibles were made from 1/2- by 1/2- by 3/8-inch thick blocks (W, Ta) or 5/8-inch-diameter by 3/8-inch-thick cylinders (TaB_2, TaC, and HfC) and had 1/4-inch-deep cavities with threaded walls. The threads provided a sensitive area for detecting reaction with the molten UO_2. Electric-discharge machining was employed for the cavitation and the threading of the crucibles. The blocks were cut from bar stock, and the cylinder blanks were produced by hot pressing the finely powdered materials in graphite dies. The hot-pressing procedure was the same as that employed in reference 2 except that two-way load application was used. Figure 1 shows a tantalum crucible loaded with UO_2. Table III gives the densities of the crucibles, the particle size of the hot-pressed powders, and the hot-pressing conditions employed.

APPARATUS

Figure 2 shows the furnace used to heat the crucibles for the compatibility study. The furnace is heated inductively by a 50-kilowatt 9600-cycle-per-second motor generator. The induction coil is radially and axially centered between an outer ($4\frac{1}{2}$-in. diam.) Pyrex tube and an inner ($3\frac{1}{2}$-in. diam.) fused quartz tube that forms the furnace chamber. Cooling water is circulated within the induction coil and through the annular passage between the tubes.

The furnace is mounted on and supported by a 4-inch oil-diffusion pump backed by a mechanical pump. The chamber pressure is indicated by two gages, one for the range of 0 to 25 microns, and the other for the range from 0 to 800 millimeters of mercury.

Because vapors and films deposited on the prism face (in spite of the prism cover) would interfere with optical pyrometer readings, the specimen temperature during the test was established by careful calibration of the coil voltage against furnace temperature. The following steps were used to make this calibration:

(1) The optical pyrometer and prism assembly was calibrated against a National Bureau of Standards certified standard lamp.

(2) A curve of temperature against power was made by sighting on a tungsten specimen placed in the test position. The specimen approached blackbody conditions. Tungsten was used because it has low volatility.

(3) The calibration was checked in the furnace against the melting points of columbium (4474° F, ref. 3, p. 346), molybdenum (4710° F, ref. 4, p. 355), zirconium dioxide (4870° F, ref. 4, p. 356), uranium dioxide (5000° F, ref. 5), and tantalum (5430° F, ref. 4, p. 355). These checks substantiated the belief that the temperature was accurate within ±50° F.

The test temperature employed, 5220° F, was dictated by furnace life, since operation at temperatures above this point resulted in excessive vaporization of the beryllia radiation shield holders and subsequent movement of the tungsten radiation shields. At the end of the program, however, one run at 5500° F was made on a tungsten crucible with a UO_2 charge.

PROCEDURE

From the previous investigation (ref. 1) it was known that the evaporation rate of UO_2 at high temperature in vacuum was such that a small sample would be lost before its melting point was reached. Therefore, for this study, use of an inert gas blanket was necessary to suppress the vaporization of UO_2. Since the furnace was originally designed for vacuum work, it was necessary that inert gas pressures above atmospheric pressure be avoided. A starting static argon pressure of 400 millimeters of mercury and a time of 15 minutes were the test conditions established by a few preliminary furnace runs. Tungsten crucibles with UO_2 charges were used to ascertain that at 5220° F for 15 minutes the pressure rose to less than 600 millimeters when starting with a static argon pressure of 400 millimeters of mercury and that less than half the UO_2 charge was lost because of evaporation.

For the tests proper, a crucible of the test material containing approximately 1 gram of UO_2 fragments was placed on a tungsten or thoria platform within the 1-inch-diameter tungsten reaction cup. Thoria platforms were used for the two carbides and the diboride since these compounds would react with tungsten, as discovered in previous work at this Center. After the cup was placed in the furnace, the furnace was evacuated to about 2×10^{-5} millimeter of mercury and blanked off. At this point, high-purity argon (99.995 percent) was bled into the furnace until a static pressure of 400 millimeters of mercury was attained.

The furnace was brought to test temperature in a period of about 45 minutes. The pressure was closely watched during this period for abrupt changes that might indicate reaction but none were noted. When the voltage setting corresponded to the test temperature of 5220° F, the power was held constant for a period of 16 minutes. The furnace temperature stabilized within 1 minute, and the actual time at the test temperature was 15 minutes. Pressure observations as well as gross temperature readings were also made during this 15-minute period. At its conclusion the power was decreased over a period of 45 minutes, which was the same rate as that followed in the heating cycle.

The crucibles were sectioned vertically after the test, and both halves were mounted in bakelite so that the cross sections could be ground and polished. Figure 3 shows a cross section of a tungsten crucible and its UO_2 contents.

After surface preparation, the cross sections were examined under the metallurgical microscope in both unetched and etched conditions.

Photomicrographs were taken of regions where reactions had occurred, and these areas were subsequently investigated by means of X-ray diffraction analyses, microhardness measurements, and electron-beam microanalyses (see appendix). X-ray diffraction analyses were also made of the entire cross sections.

A microhardness tester with a Knoop diamond indenter was used to measure the hardness of parent UO_2, parent crucible materials and also any new phases present. The average values of ten readings were used in making comparisons. Since Knoop hardness number depends on the load employed (ref. 6), only hardness results obtained under the same load can be compared.

RESULTS AND DISCUSSION

Tungsten

X-ray diffraction analyses of the crucible cross sections did not indicate the presence of any new phases, but an X-ray scan of the UO_2 meniscus surface showed metallic tungsten to be present in addition to the UO_2. This result and the results of the aforementioned physical methods indicate that molten UO_2 does react with tungsten at the test temperature of 5220° F.

Figure 4 is a photomicrograph of a cross-sectional segment of the UO_2 meniscus. The gray UO_2 supports a thin white layer that is approximately 0.001 inch thick. This layer consists of two phases, a white matrix and a gray dispersed phase. Knoop microhardness measurements were made on this thin layer and on the parent tungsten and UO_2. It was necessary to use a 5-gram load so that the microhardness impressions could be accommodated by the thin layer. The impressions obtained were not confined to just one phase of the layer but encompassed areas of both gray and white phases. The microhardness of the white layer, 557, fell between that of tungsten, 338, and UO_2, 693. These microhardness measurements in combination with the structure and X-ray diffraction evidence indicate that the white layer is a mechanical mixture of UO_2 and tungsten. Comparison of the after-test and the as-received hardnesses of the parent materials did not indicate any significant change.

A typical photomicrograph of the tungsten crucible cross section in the region of a thread apex is presented as figure 5(a). The gray material that can be seen to have penetrated this and other threads along grain boundaries was identified as UO_2 by electron-beam microanalysis.

The results of the run with tungsten and UO_2 at 5500° F were essentially the same as those for the run at 5220° F, but one additional indication of reaction was found as shown in figure 5(b), a photomicrograph of the crucible cross section in the bottom region at the interface of tungsten and molten UO_2. The gray UO_2 (upper portion of the figure) contains several white droplets, all of which were too small for microhardness determination. These droplets are thought to be tungsten.

From these results it appears that molten UO_2 attacks tungsten. The suggested reaction mechanism is the solution of tungsten in the molten UO_2 while at the test temperature, followed by the precipitation of the dissolved tungsten at the UO_2 melt meniscus and within the UO_2 melt during the cooling period.

Similar results were reported in an investigation of the compatibility of molten alumina with tungsten crucibles heated in vacuum and in argon (ref. 7). In both cases the alumina melt contained metallic tungsten, and alumina had penetrated the tungsten grain boundaries. Metallic tungsten was also found at the melt meniscus when the crucible was heated in argon. The reaction mechanism that was suggested in reference 7 involved the dissolution of a tungsten-bearing species by the intergranular attack of molten alumina on the tungsten. It was then postulated that this tungsten-bearing species be in equilibrium with a vapor that readily decomposes into tungsten metal and some other constituent. In vacuum, where the mean free path is large, the tungsten-bearing species and/or its decomposition products would be carried away and no tungsten film would form on the alumina melt meniscus. But in an inert atmosphere where the mean free path is small, the tungsten is reflected back to the melt surface where it precipitates.

Tantalum

No new phase was found in the tantalum crucible cross sections by X-ray diffraction analysis. A reaction did occur, however, as evidenced by the condition of the crucible threads and the bottom as shown in figure 6. The gray UO_2 contains several white particles that were identified as metallic tantalum by electron-beam microanalysis. Knoop microhardness measurements were made on some of the large white particles in the UO_2 and on the parent tantalum and UO_2. The hardness of the parent UO_2 had not changed significantly, but the hardness of the parent tantalum had increased almost 80 percent over that of the material in the as-received condition. In turn, the white tantalum particles were more than 40 percent harder than the parent tantalum.

One more observation is worthy of note. Metallographic examination of one of the crucible cross sections revealed a white dendritic formation in the gray UO_2 near the meniscus as shown in figure 7. This dendritic formation would indicate a melting point for the white material above that of UO_2. Electron-beam microanalysis identified the dendrites as tantalum.

As in the case for the tests with tungsten and molten UO_2, a solution-precipitation type of reaction mechanism is suggested. Another possible mechanism is the melting of tantalum as a result of a lowering of the tantalum melting point by solution of oxygen. The melting point of columbium, the sister element of tantalum, is lowered approximately 200° F by a 1-percent oxygen content (ref. 3, p. 513). Solution of oxygen would explain the increase in the hardness of the parent tantalum and the still higher hardness of the white particles, which are assumed to be tantalum. It is reported (ref. 3, p. 603) that small amounts of oxygen increase the hardness of tantalum considerably. The oxygen could be available for solution as a result of the partial decomposition of UO_2 at its melting point as reported in reference 8. To make certain that the true melting point of tantalum (5430° F, ref. 4) was not reached during test, the furnace-temperature calibration was checked and found to be accurate. A test run was also made in which a tantalum specimen was heated alone to the test temperature of 5220° F; there were no signs of melting.

Tantalum Diboride

The entire UO_2 charges were consumed by reaction with the TaB_2 crucible. Reaction was also indicated from metallographic examination of the polished crucible cross sections. The crucible cross section with two TaB_2 threads that have undergone some degradation is shown in figure 8. In addition, a second phase had appeared at the grain boundaries.

No uranium compound was found by X-ray diffraction analyses of the crucible cross sections, but there were some indications of the presence of tri-tantalum tetraboride (Ta_3B_4), which indicated a loss of boron.

Further evidence of boron loss was the change in the lattice parameters of the TaB_2 phase. The X-ray diffraction analyses were as follows:

	As received	After test	Theoretical
Lattice parameter, A:			
a	3.09	3.10	3.078 (ref. 4, p. 293)
c	3.24	3.23	3.265 (ref. 4, p. 293)
Boron subscript	1.9	1.8	2.0

The change in the lattice parameters indicates a loss of boron (ref. 4, p. 293), which means a reduction of the boron subscript from 1.9 to 1.8. The tantalum diboride $TaB_{1.8}$ is near the lower limit for the tantalum diboride homogeneity range, $TaB_{1.78}$ to $TaB_{2.57}$, as established by Kiessling in reference 4 (p. 293).

From the tentative equilibrium diagram of the tantalum-boron system as proposed by Kieffer and Benesovsky in reference 3 (p. 552), the tantalum diboride $TaB_{1.9}$ when heated to the 5220° F test temperature would enter a liquid plus TaB_2 region. Loss of boron while heating has been reported (ref. 9, p. 175) that would move the diboride composition toward the tantalum-rich side of the phase diagram. It is proposed that on cooling from the liquid plus TaB_2 region enough boron had been lost so that the 4750° F isotherm separating the liquid plus TaB_2 region from the TaB_2 plus Ta_3B_4 region is intersected. This intersection would result in the coprecipitation of Ta_3B_4 and TaB_2 of the limiting composition and explain the presence of the second phase in figure 8.

Microhardness measurements made on the TaB_2 crucible after the test were in agreement with the values before the test.

In evaluating the results, reference is made to the findings of the previous investigation (ref. 1) in which it was found that TaB_2 reacts with UO_2 at 4000° F and above and results in slight adherence and the formation of uranium diboride (UB_2). Since the degree of reaction was slight even at 5000° F, TaB_2 was included in the present study. That no UB_2 was found by X-ray diffraction analysis of the crucible cross section is understandable since the UB_2 formed would probably evaporate rapidly at the test temperature, which is 895° F above the melting point of UB_2, 4325° F (ref. 10). The reaction between molten UO_2 and TaB_2

at 5220° F can then be described as resulting in the formation of UB_2, which is augmented by free boron evolved from the partial decomposition of the TaB_2 phase.

Tantalum Carbide

Reaction between the TaC crucible and its molten UO_2 charge resulted in the complete consumption of the UO_2. No uranium compound was found by X-ray diffraction analysis of the crucible cross sections, but there was evidence that carbon was lost from the TaC. A summary of visual observations, microhardness measurements, and X-ray diffraction analyses is presented in the following table:

Property	Experimental values		Literature values
	As received	After test	
Lattice parameter, A	4.455	~4.44	4.457 (ref. 11)
C-Ta atom ratio from lattice parameter values	1.0 (ref. 11)	~0.88 (ref. 11)	1.0 (ref. 11)
Knoop microhardness (5g load), kg/sq mm	1876	3990	1952 (ref. 4, p. 120)
Color	Gold	Silver	----------

Loss of carbon was indicated by a decrease in the lattice parameter of the TaC crucible material from 4.455 to approximately 4.44 angstroms. Such a decrease corresponds to a lowering of the atom ratio of carbon to tantalum from 1.0 to approximately 0.88 according to an investigation on the variation of lattice parameter with carbon content of TaC (ref. 11). Such carbon losses with accompanying lattice contractions have been observed for TaC when it is heated to high temperatures in 1 atmosphere of helium (ref. 12). In the present case, somewhat greater contractions in the lattice than those in reference 12 were obtained because perhaps of a lesser pressure of inert gas (400 compared with 760 mm), which might be less effective in inhibiting the TaC decomposition.

Accompanying the loss of carbon by the TaC crucible were color and microhardness changes. The TaC crucible lost its gold color, which is characteristic of tantalum carbides with carbon-tantalum atom ratios of 0.9 or greater (ref. 11, p. 1596) and became silver in color. The

Knoop microhardness more than doubled, increasing from 1876 to 3990 kilograms per square millimeter. In a current investigation at the Lewis Center, substoichiometric tantalum carbides have exhibited much higher microhardnesses than the stoichiometric carbide.

As in the case for the TaB_2, the previous results must be evaluated in the light of the findings of reference 1 in which TaC reacted with UO_2 at a temperature as low as 4500° F to form uranium carbide (UC). Since the reaction was not extensive, even at 5000° F, TaC was included in this study. The hypothesis advanced in the previous investigation is that the free carbon made available by the decomposition of TaC was the coreactant in the formation of UC. The higher temperature employed in the present investigation would then result in accelerated rates of decomposition of TaC and formation of UC. The fact that no UC was found in the TaC crucible after the test is probably a result of the high evaporation rate of UC at the test temperature, which is 730° above the melting point of UC, 4490° F (ref. 4).

Hafnium Carbide

An amount of UO_2 remained in the HfC crucibles after testing that was comparable to that remaining in the tungsten and tantalum crucibles after testing. Some reaction did occur as evidenced by visual observation of the crucibles during the test and by the physical-measurement methods. It is necessary to refer to the two HfC crucibles tested separately since the results of their analyses are complementary.

The first compatibility run was stopped after only 2 minutes at the test temperature of 5220° F because of a bubbling action at the surface of the molten UO_2, which was viewed by an optical pyrometer. No such action was observed for the second run.

Metallographic examination of the crucible cross sections revealed a considerable quantity of white particles at the UO_2 meniscuses and within the UO_2 as shown in figures 9 and 10. Figure 9(a) shows a part of the UO_2 meniscus for the short-test-time crucible that is composed of white particles dispersed in a gray UO_2 matrix with a large area of gray UO_2 beneath. Figures 9(b) and 10 show the UO_2 meniscus and a thread apex region, respectively, of the full-test-time crucible. The meniscus in figure 9(b) contains somewhat larger white particles strung together, with more of these particles dispersed below the meniscus. Figure 10 shows a sawtooth structure that developed at the thread

profile and some white particles dispersed in the UO_2. Electron-beam microanalysis of the numbered areas in figures 9(a) and 10 are given in the following table:

Figure	Area	Identification
9(a)	1	HfC
	2	UO_2
	3	HfC
	4	HfC
	5	UO_2-Hf (85 wt. percent U, 5-10 wt. percent Hf)
10	1	HfC
	2	UO_2
	3	UO_2-Hf (65 wt. percent U, 25 wt. percent Hf)
	4	HfC

In figure 9(a) the small white particles in the meniscus band and the thin layer separating the band from the remainder of the UO_2 below (areas 1, 3, and 4) are identified as HfC. Although there appear to be two phases making up the thin layer, only HfC was reported for both the top and the bottom. Areas 2 and 5, as expected, are identified as UO_2; however, area 5 contains 5 to 10 weight percent hafnium in solution. For figure 10, the results were the same; areas 1 and 4 were identified as HFC, while areas 2 and 3 were identified as UO_2, the latter contained 25 weight percent hafnium.

X-ray diffraction analyses were run on the meniscus surfaces of segments of UO_2 broken out of the crucible cross sections and on a crucible bottom and a crucible cross section. These analyses are summarized in the following table:

HfC crucible	Area	Phase detected		
		Major (>> 10 percent)	Secondary (≈10 percent)	Minor (<< 10 percent)
Short test time	Top of meniscus	UO_2, HfC, UB_4	HfB_2, UC	HfO_2
Full test time	Top of meniscus	HfC	UO_2	----
	Crucible bottom	HfC, HfB_2	--------	----
	Crucible cross section	HfC	--------	HfB_2

For the short-test-time run, UO_2, HfC, and UB_4 phases have been found as major, HfB_2 and UC phases as secondary, and hafnium dioxide (HfO_2) as a minor phase on the UO_2 meniscus. For the full-test-time run, only HfC was found as a major phase on the UO_2 meniscus, and UO_2 was present as a secondary phase. On the crucible bottom, HfB_2 was found as a major phase in addition to HfC, and in the parent HfC crucible cross section, HfB_2 was found as a minor phase.

Although chemical analysis indicated the presence of 0.72 percent boron in the starting HfC crucible, X-ray diffraction analysis and metallographic examination did not indicate the presence of any second phase. The test run, however, apparently resulted in the formation of HfB_2 as evidenced by the post-test X-ray analyses given in the previous table and by metallographic examination of the crucible cross sections. In figure 10 can be seen a second phase of small white grains at the HfC grain boundaries and within the HfC grains. A comparative measurement was made of the area occupied by the white phase, and if it is assumed to be HfB_2, it is equivalent to 4.5 weight percent. This value is comparable to the 6.7 weight percent HfB_2 computed, if complete reaction of the original 0.72 percent boron content is assumed. It has been shown that regardless of the proportions in which titanium or zirconium is mixed with boron and carbon, the mixture when heated below 5160° F will always contain the diboride of the respective metal at the expense of a carbide phase (ref. 13, p. 395). Since hafnium is in the same periodic group as titanium and zirconium, it may be assumed to have reacted similarly, as is indicated by the compatibility run.

Microhardness measurements were made on the parent crucible material and on parent UO_2 and indicated that while the HfC hardness had not changed, the hardness of the UO_2 had doubled. This increase may be explained by the solution of hafnium or a hafnium compound in the UO_2 as determined by the electron-beam microanalysis. Attempts to measure the microhardness of the white particles in the UO_2 and the second phase in the HfC were unsuccessful because the indentations obtained were asymmetrical. The second phase, however, did appear harder than the HfC matrix.

In evaluating the results, reference is again made to the findings of reference 1. It was determined that UO_2 and HfB_2 react extensively at 4700° F to form a liquid phase in which only the original materials can be detected by X-ray diffraction analysis. In comparison, HfC was completely inert toward UO_2 up to 5000° F. For the present case then, some reaction can be expected between the molten UO_2 and the HfB_2 that

formed in the HfC crucible. This reaction may be responsible for the solution of hafnium in the molten UO_2 creating a HfC crucible surface condition such as shown in figure 10.

The bubbling disturbance noted at the molten UO_2 surface of the first run is attributed to the 7.4-percent porosity of this short-test-time crucible compared with the 1.7-percent porosity of the full-test-time crucible. Because of this porosity, the extent of the molten UO_2 - HfB_2 reaction would be greater and a larger quantity of reaction products would be evolved, which would account for the bubbling at the molten UO_2 surface. Since the test involving the porous crucible was stopped, some of the relatively low-melting-point, high-vapor-pressure reaction products, uranium tetraboride (UB_4) and UC were retained. Their absence at the UO_2 meniscus of the less porous crucible is then the result of less reaction-product formation and the complete vaporization of what did form.

CONCLUDING REMARKS

From the investigation of the compatibility of uranium dioxide with tungsten, tantalum, tantalum diboride, tantalum carbide, and hafnium carbide, it appears that neither tantalum diboride nor tantalum carbide would be feasible as a component in a nuclear reactor fuel element where there would be contact with molten uranium dioxide. The use of tungsten, tantalum, and hafnium carbide for some limited time, however, does seem to be possible; tungsten is the most likely candidate. It should be remembered that the data reported herein are for materials of a given analysis and that the tests were conducted under certain fixed conditions. Possibly, at lower temperatures and higher pressures, the reactions would be less severe. Lastly, the boron impurity in the hafnium carbide appears to be partly responsible for the molten uranium dioxide - hafnium carbide reaction, and a higher purity carbide may well be more compatible with molten uranium dioxide.

Lewis Research Center
National Aeronautics and Space Administration
Cleveland, Ohio, August 21, 1962

APPENDIX - METHOD OF ELECTRON-BEAM MICROANALYSIS

The concentration determinations were performed by Advanced Metals Research Corporation, Somerville, Massachusetts with the AMR electron-beam microanalyzer. A beam of electrons is accelerated with a high pctential and focused by means of electromagnetic lenses to a diameter of about 1 to 2 microns at the surface of the specimen to be examined. As in an X-ray tube, the specimen will act as a primary source of X-rays characteristic of the elements excited by the electron beam. A chemical analysis of the excited area is afforded by analysis of the characteristic X-ray lines by means of a single-crystal X-ray spectrometer.

A curved mica-crystal focusing goniometer employing a helium path and a flow-proportional counter was set up to record the characteristic X-ray lines of the crucible materials and uranium dioxide. Elements below atomic number 11 were not analyzed for in this case because of the difficulties in dispersing or diffracting the long wavelength radiation resulting from their excitation. Therefore, for the hafnium carbide crucible and for any uranium dioxide analyses, only the hafnium and uranium metal characteristic X-ray lines were recorded.

A typical analysis was performed as follows: The electron beam was positioned on the crucible matrix and the spectrometer alined for a characteristic X-ray line of the spectrum produced. Then the beam was positioned on each of the areas to be examined, while the available intensity was recorded on a chart. The beam was then positioned on the uranium dioxide melt, and the spectrometer was alined for a characteristic uranium line of the spectrum produced. The beam was again positioned on each of the areas to be examined, while the available intensity was recorded on a chart. The calculated concentrations for the cases in which alloying had occurred ($HfC-UO_2$) are taken from theoretical calculations that involve the literature values for absorption coefficients of the wavelengths measured. These calculations, in general, are only precise to ±10 percent of the amount present.

REFERENCES

1. Gangler, James J., Sanders, William A., and Drell, Isadore L.: Uranium Dioxide Compatibility with Refractory Metals, Carbides, Borides, Nitrides, and Oxides Between 3500° and 5000° F. NASA TN D-262, 1960.

2. Sanders, William A., and Grisaffe, Salvatore J.: The Hot-Pressing of Hafnium Carbide (Melting Point, 7030° F). NASA TN D-303, 1960.

3. Miller, G. L.: Tantalum and Niobium. Butterworths Sci. Pub., 1959.

4. Schwarzkopf, P., and Kieffer, R.: Refractory Hard Metals. The Macmillan Co., 1953.

5. Wisnyi, L. G., and Pijanowski, S. W.: The Thermal Stability of Uranium Dioxide. KAPL-1702, Knolls Atomic Power Lab., Nov. 1, 1957. (Available from Office of Tech. Services, U.S. Dept. Commerce, Washington, D.C.)

6. Bückle, H.: Microhardness Testing in Powder Metallurgy. Powder Metallurgy, Intersci. Publ., 1961, pp. 221-249.

7. Hasapis, A. A., Panish, M. B., and Rosen, C. L.: The Vaporization and Physical Properties of Certain Refractories. Pt. 1. Techniques and Preliminary Studies. TR 60-463, WADD, Oct. 1960.

8. Anderson, J. S., et al.: Decomposition of Uranium Dioxide at Its Melting Point. Nature, vol. 185, no. 4717, Mar. 26, 1960, pp. 915-916.

9. Brewer, Leo, Sawyer, Dwight L., Templeton, D. H., and Dauben, Carol H.: A Study of the Refractory Borides. Jour. Am. Ceramic Soc., vol. 34, no. 6, June 1951, pp. 173-179.

10. Howlett, B. W.: A Note on the Uranium-Boron Alloy System. Jour. Inst. Metals, vol. 88, no. 2, Oct. 1959, pp. 91-92.

11. Bowman, Allen L.: The Variation of Lattice Parameter with Carbon Content of Tantalum Carbide. Jour. Phys. Chem, vol. 65, no. 9, Sept. 1961, pp. 1596-1598.

12. Kempter, Charles P. and Nadler, M. R.: Thermal Decomposition of Niobium and Tantalum Monocarbides. Jour. Chem. Phys., vol. 32, no. 5, May 1960, pp. 1477-1481.

13. Glaser, Frank W.: Contribution to the Metal-Carbon-Boron Systems. AIME Trans., vol. 194, Apr. 1952, pp. 391-396.

14. Anon.: X-Ray Powder Data File. Spec. Tech. Publ. 48-J, ASTM, 1961.

15. Cotter, P. G., and Kohn, J. A.: Industrial Diamond Substitutes: I - Physical and X-Ray Study of Hafnium Carbide. Jour. Am. Ceramic Soc., vol. 37, no. 9, Sept. 1954, pp. 415-420.

16. Belle, J., ed.: Uranium Dioxide: Properties and Nuclear Applications. Naval Reactors, Div. Reactor Development U.S. Atomic Energy Commission, July 1961.

TABLE I. - MELTING POINTS AND ANALYSES OF AS-RECEIVED MATERIALS

Nominal material	Melting point		Combined carbon or boron[a], wt percent	Free carbon[a], wt percent	Impurities[a], percent			Calculated formula	Lattice parameters		
	°F	Ref.			0.05-0.5	0.005-0.05	< 0.01		NASA data, A	Other data	
										A	Ref.
Tungsten	6120	4, pp. 355-356	-----	----	-------	Fe	Si,Al,Cu,Ni, Cr,Mn,Ca,Mg, Mo,Co,Na,K	----------	a = 3.169	a = 3.165	14
Tantalum	5430	4, pp. 355-356	-----	----	-------	--------	Si,Al,Fe,Ca, Cu,Mg,Sr,Na, K,Li	----------	a = 3.305	a = 3.306	14
Tantalum diboride	5430 (decom-poses)	4, pp. 355-356	10.46	----	Co	Si,Fe,Cb	Al,Cu,Ni,Cr, V,Mn,Ca,Mg, Zr,Mo,Sr,Na, K,Li	$TaB_{1.9}$	a = 3.09 c = 3.24	a = 3.078 c = 3.265	4, p. 293
Tantalum carbide	7020	4, pp. 355-356	6.23	0.02	-------	Ca	Si,Al,Fe,Ti, Cu,Mg,Co,Sr, Na,K,Li	$TaC_{1.0}$	a = 4.455	a = 4.457	11
Hafnium carbide	7030	4, pp. 355-356	6.0	0.03	Zr,3.45 B,0.72 Ti,0.39	Si,Fe, Ca,Li	Al,Cu,Ni,Cr, V,Mn,Mg,Mo, Ag,Ba,Sr,Na, K	$Hf_{0.92};Zr_{0.07};Ti_{0.01}(C_{0.91};B_{0.09})$	a = 4.634	a = 4.641	15
Uranium dioxide	5000	5	-----	----	-------	Si	----------	[b]$UO_{2.02}$	a = 5.471	a = 5.473	16, p. 175

[a]Analyses supplied by National Spectrographic Laboratories, Inc., Cleveland, Ohio.

[b]Formula determined by lattice parameter from lattice-parameter - U/O atom-ratio curve found in ref. 16.

TABLE II. - KNOOP MICROHARDNESS

FOR AS-RECEIVED MATERIALS

Material	Microhardness, $k_{load\ in\ grams}$, kg/sq mm
W	k_{50} = 511
Ta	k_{200} = 136
TaB_2	k_{50} = 2833
TaC	k_5 = 1876
HfC	k_{100} = 2605
UO_2	k_{10} = 812

TABLE III. - MATERIAL DATA

Crucible material	Theoretical crucible density, percent	Powder particle size, microns	Hot-pressing conditions		
			Temperature, °F	Pressure, lb/sq in.	Time, min
Tungsten	98.2	---	----	----	--
Tantalum	98.2	---	----	----	--
Tantalum diboride	92.1	3.8	4350	4350	30
Tantalum carbide	95.2	1.7	3590	4350	30
Hafnium carbide	98.3	3.0	4640	4350	30

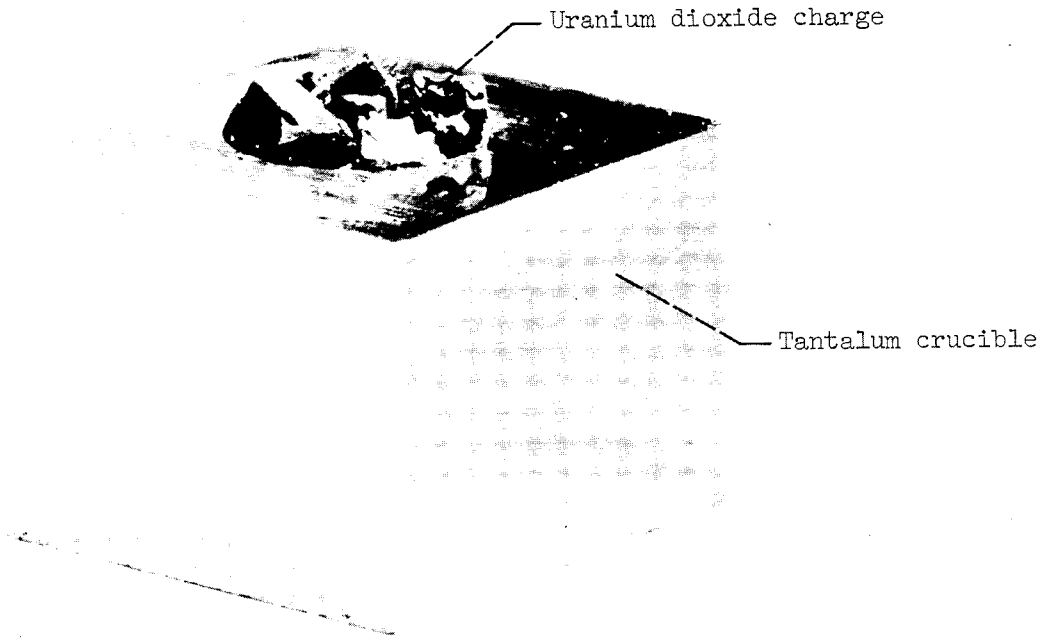

C-54116

Figure 1. - Tantalum crucible with uranium dioxide charge. X5.

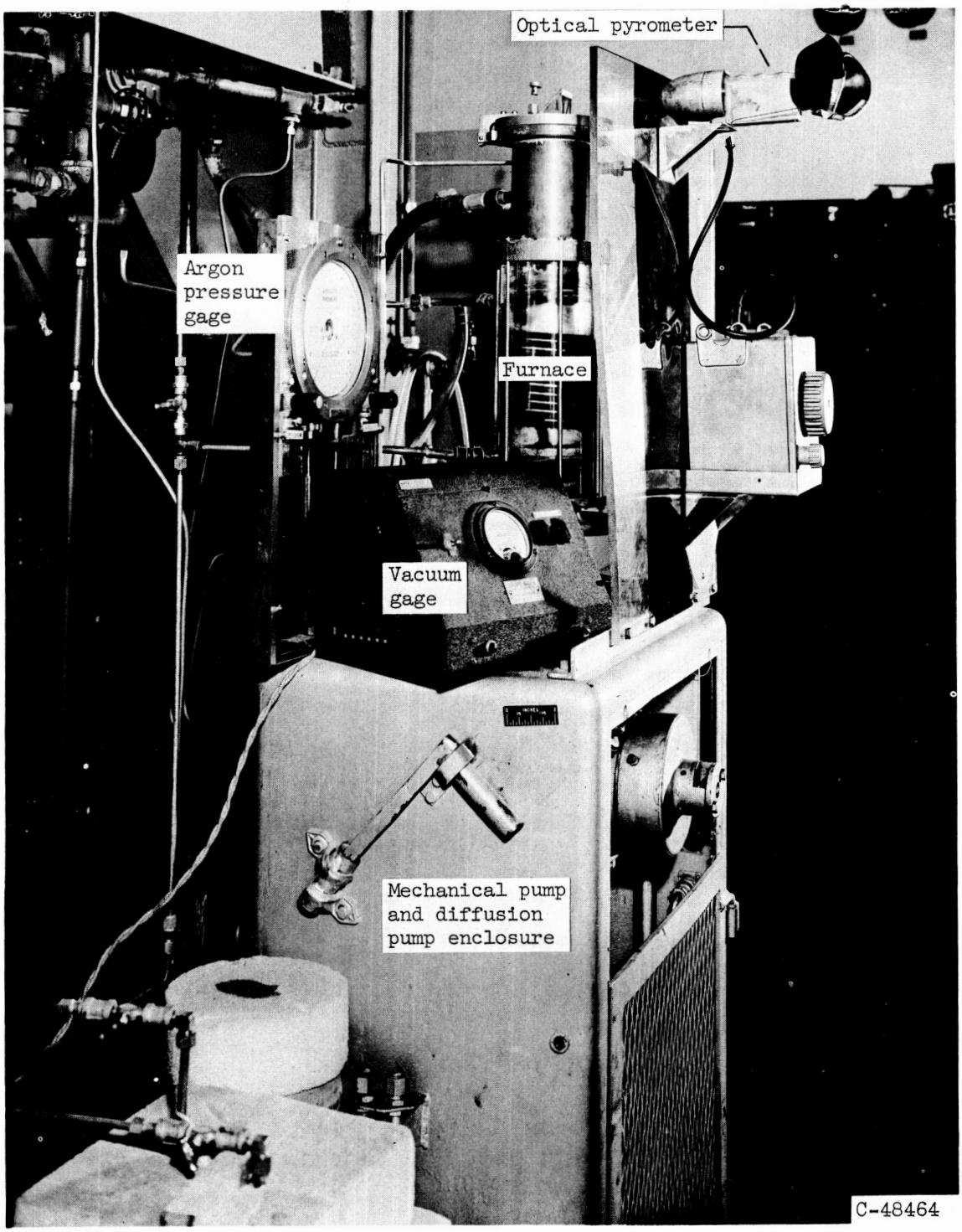

(a) Overall view.

Figure 2. - Compatibility apparatus.

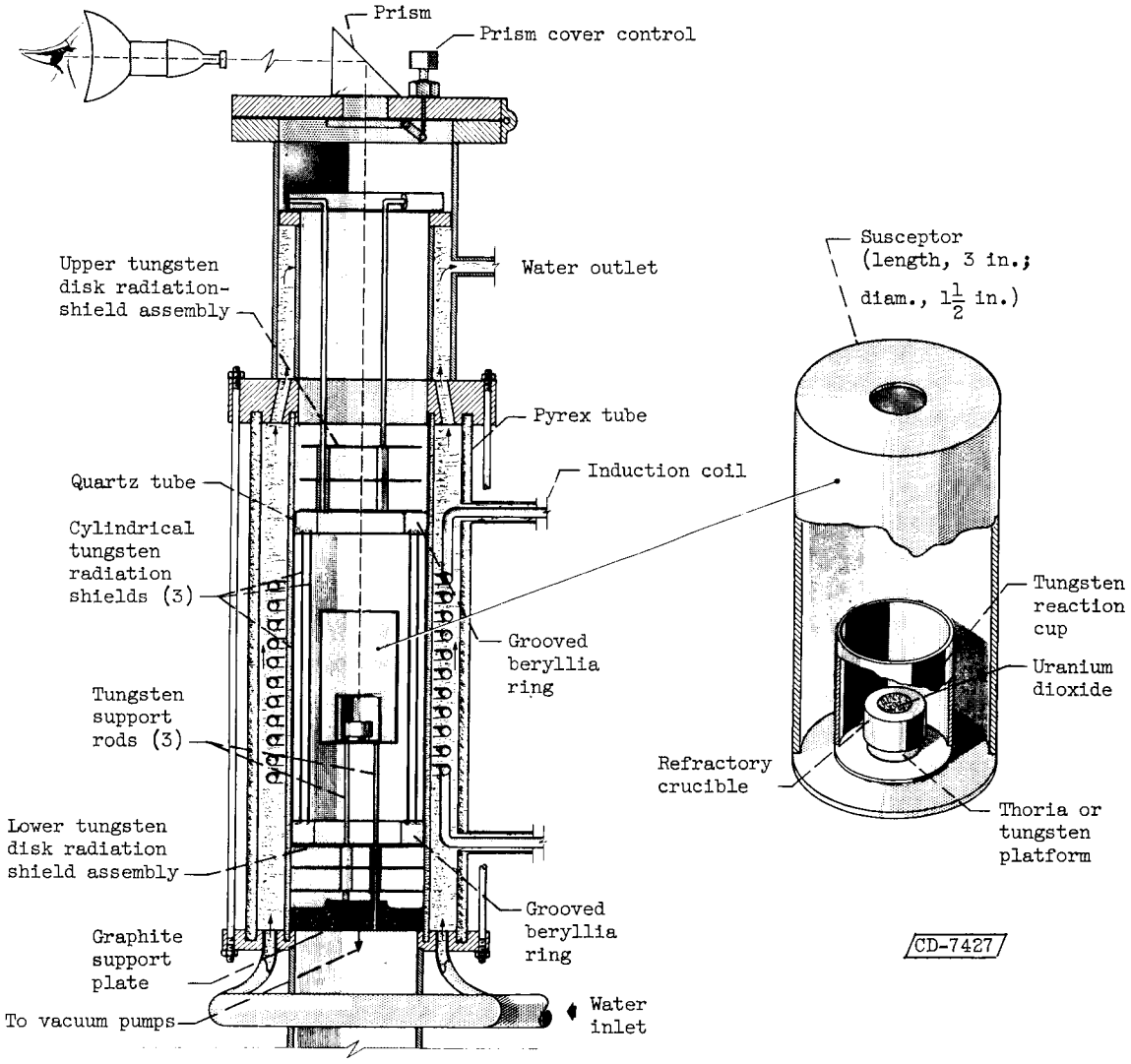

(b) Schematic of furnace.

Figure 2. - Concluded. Compatibility apparatus.

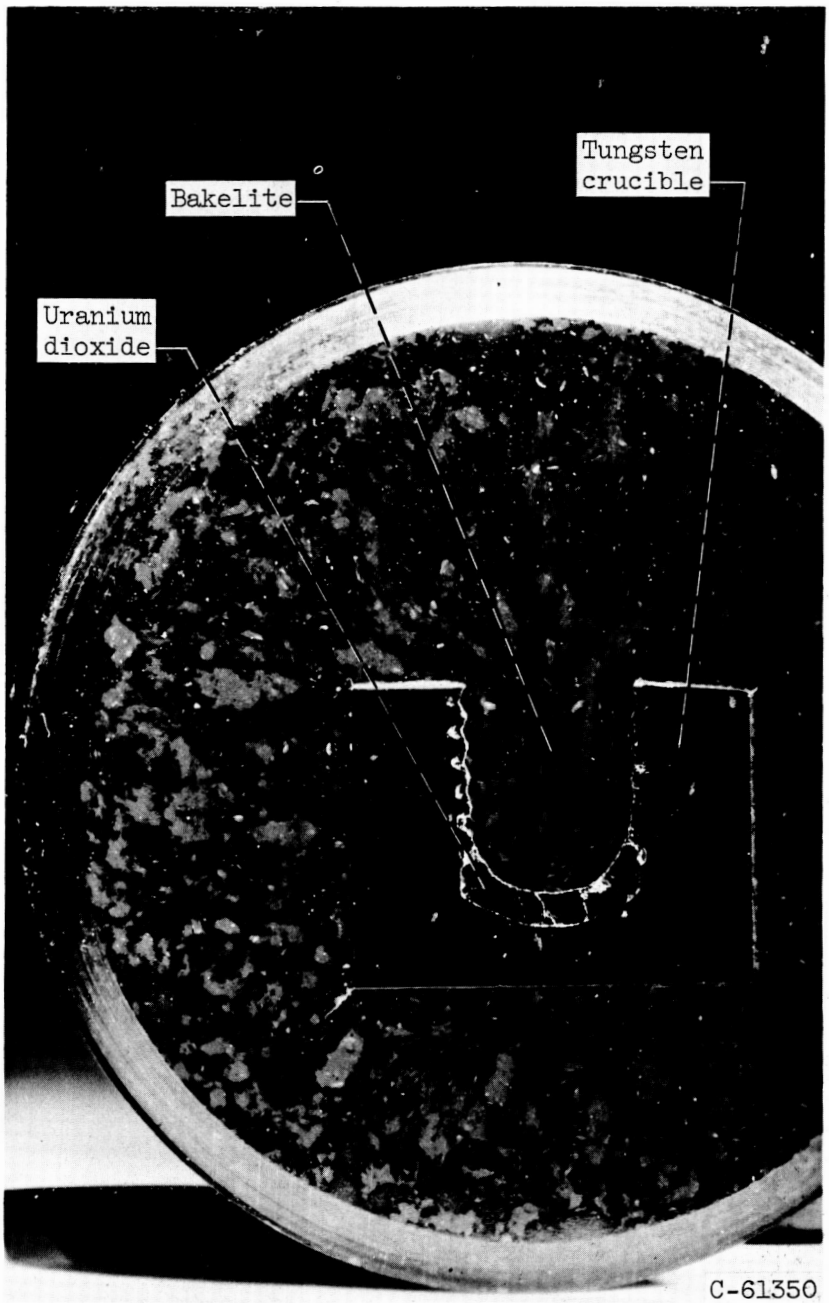

Figure 3. - Cross section of tungsten crucible with uranium dioxide contents. ×4.6.

Figure 4. - Photomicrograph of cross section of uranium dioxide meniscus region; unetched; ×1000.

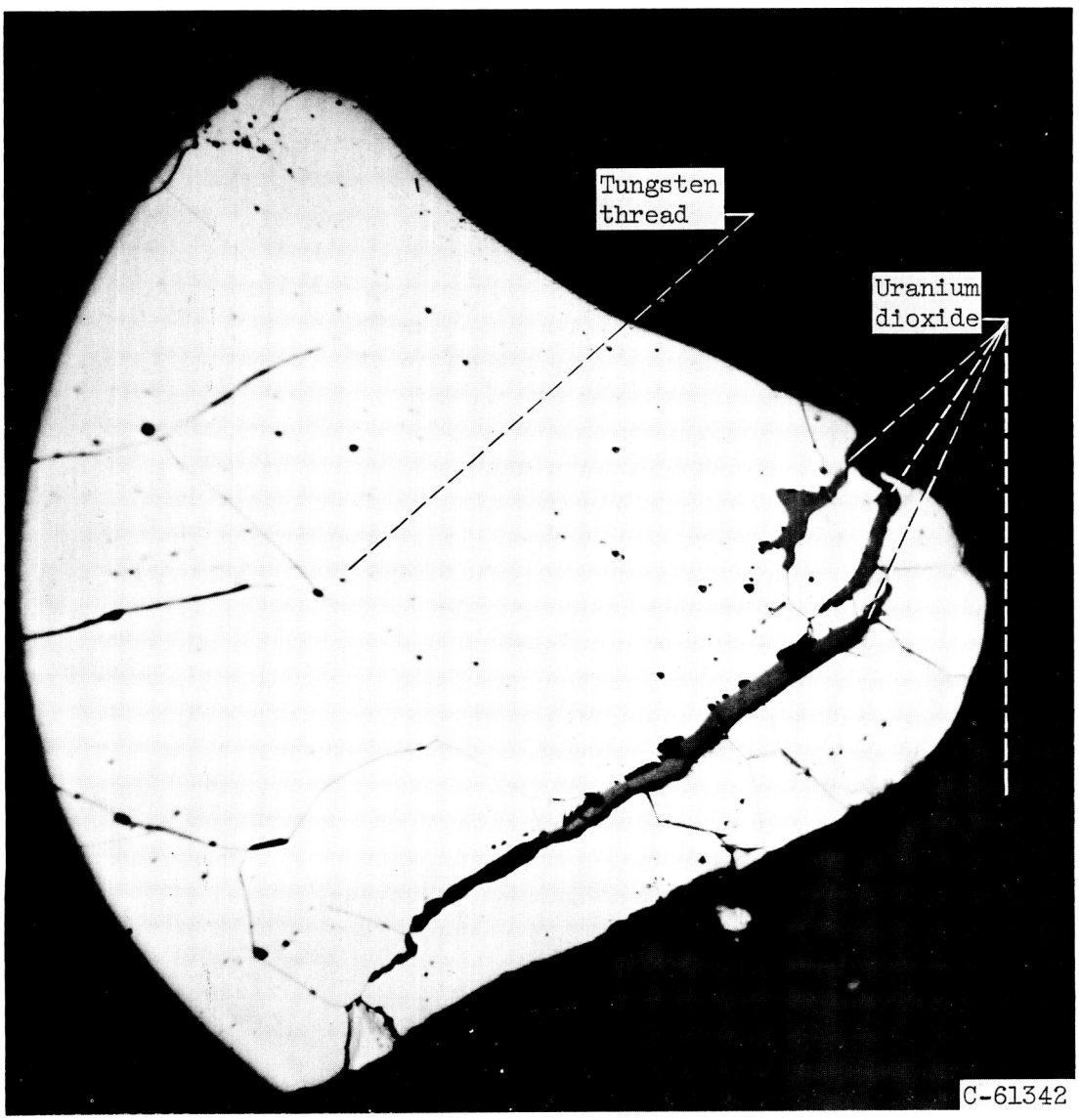

(a) Thread apex region; etchant, potassium hydroxide plus potassium ferricyanide; X500.

Figure 5. - Photomicrograph of cross section of tungsten crucible.

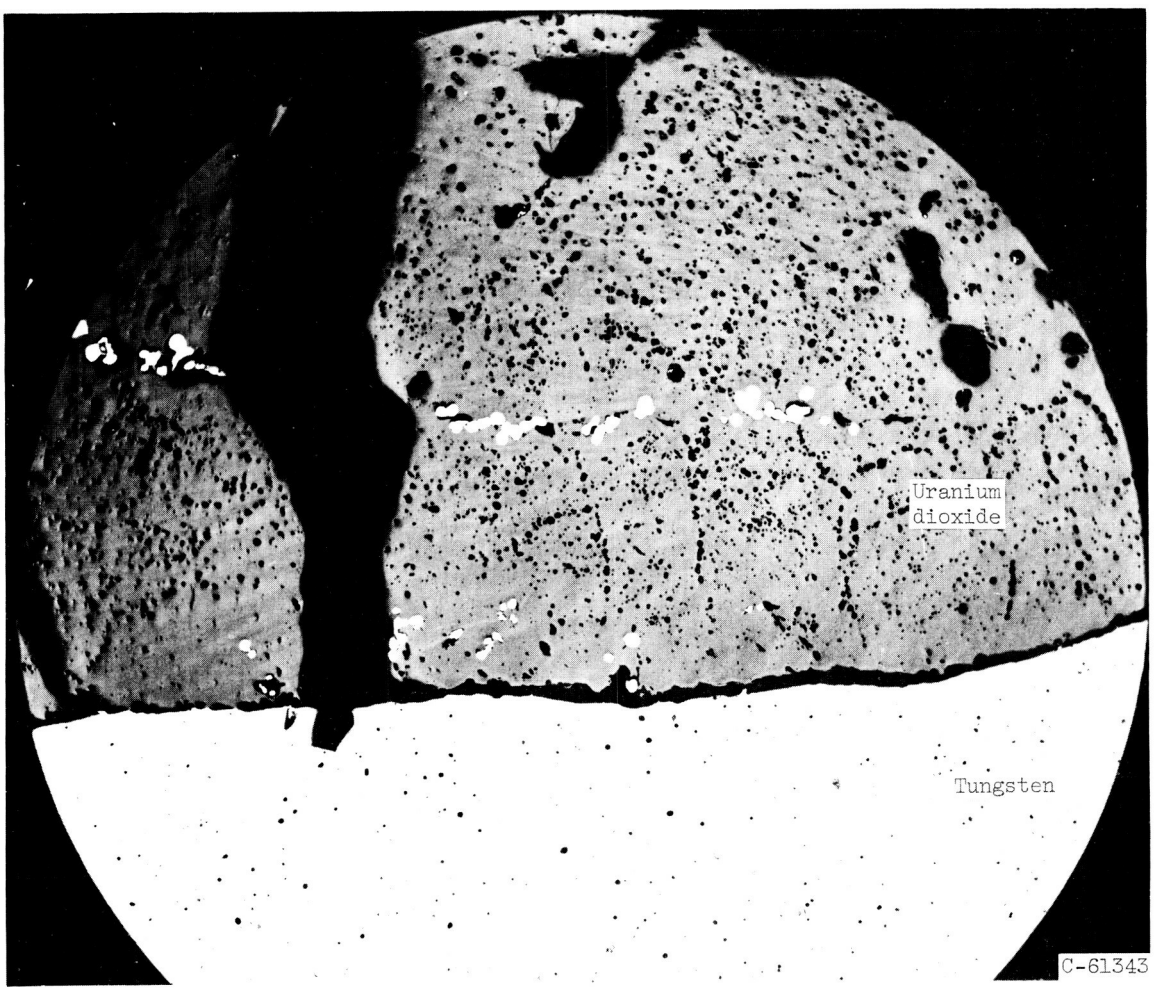

(b) Bottom region; unetched; ×150.

Figure 5. - Concluded. Photomicrograph of cross section of tungsten crucible.

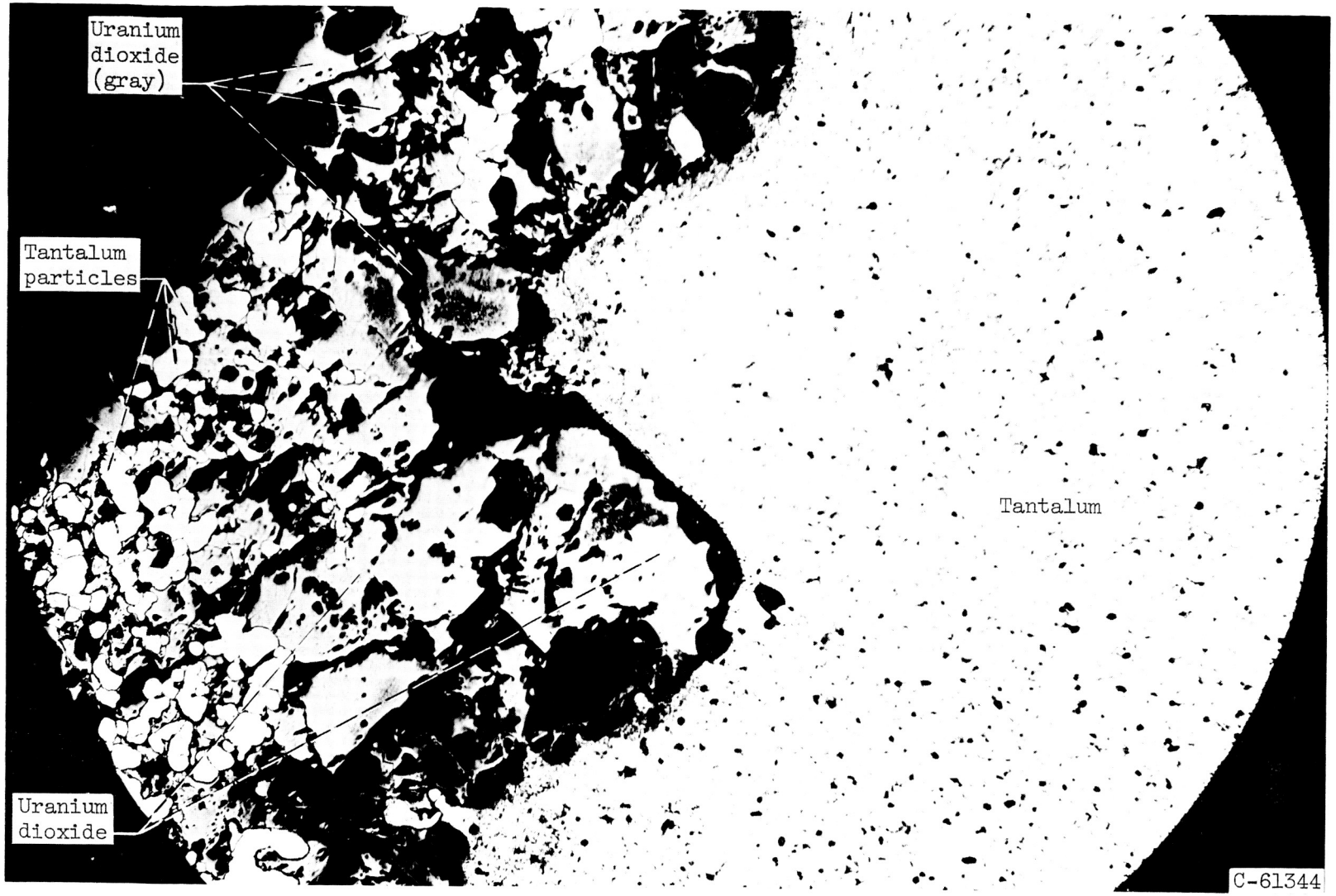

Figure 6. - Photomicrograph of cross section of tantalum crucible thread apex region; etchant, nitric acid plus hydrofluoric acid; ×100.

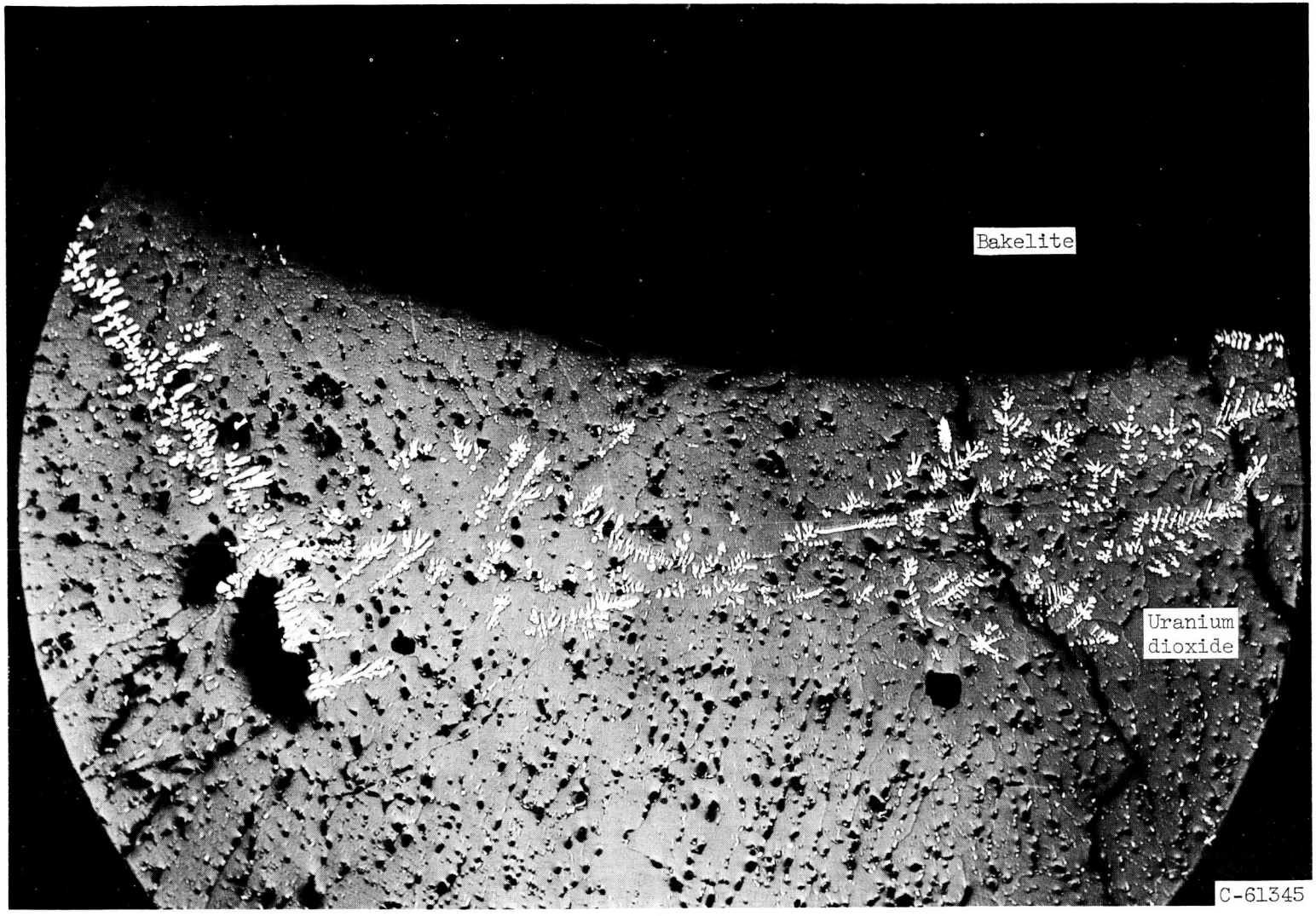

Figure 7. - Photomicrograph of cross section of uranium dioxide containing dendritric formation; etchant, nitric acid plus hydrofluoric acid; ×100.

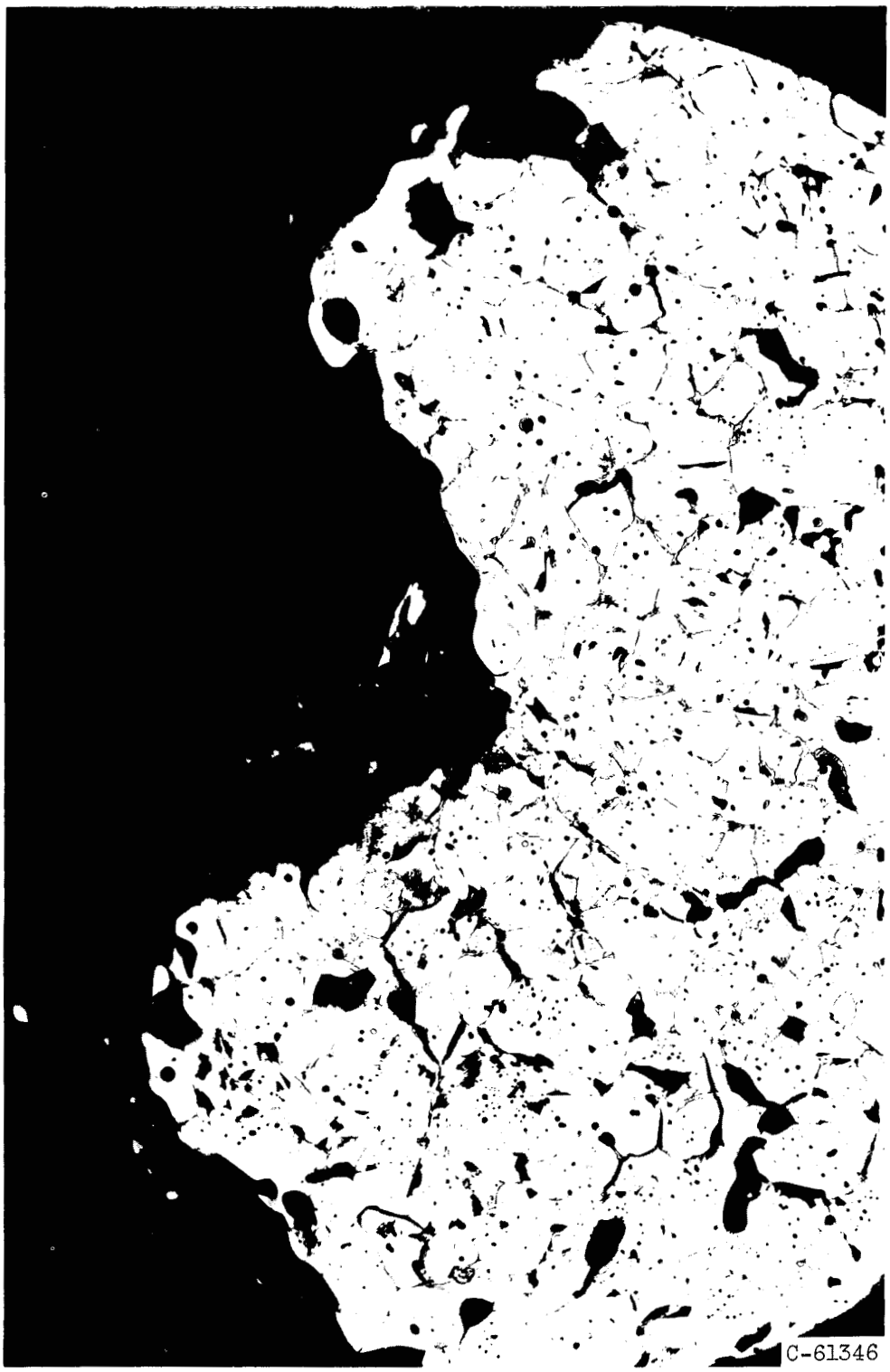

Figure 8. - Photomicrograph of cross section of tantalum diboride crucible thread region; etchant, nitric acid plus hydrofluoric acid; ×100.

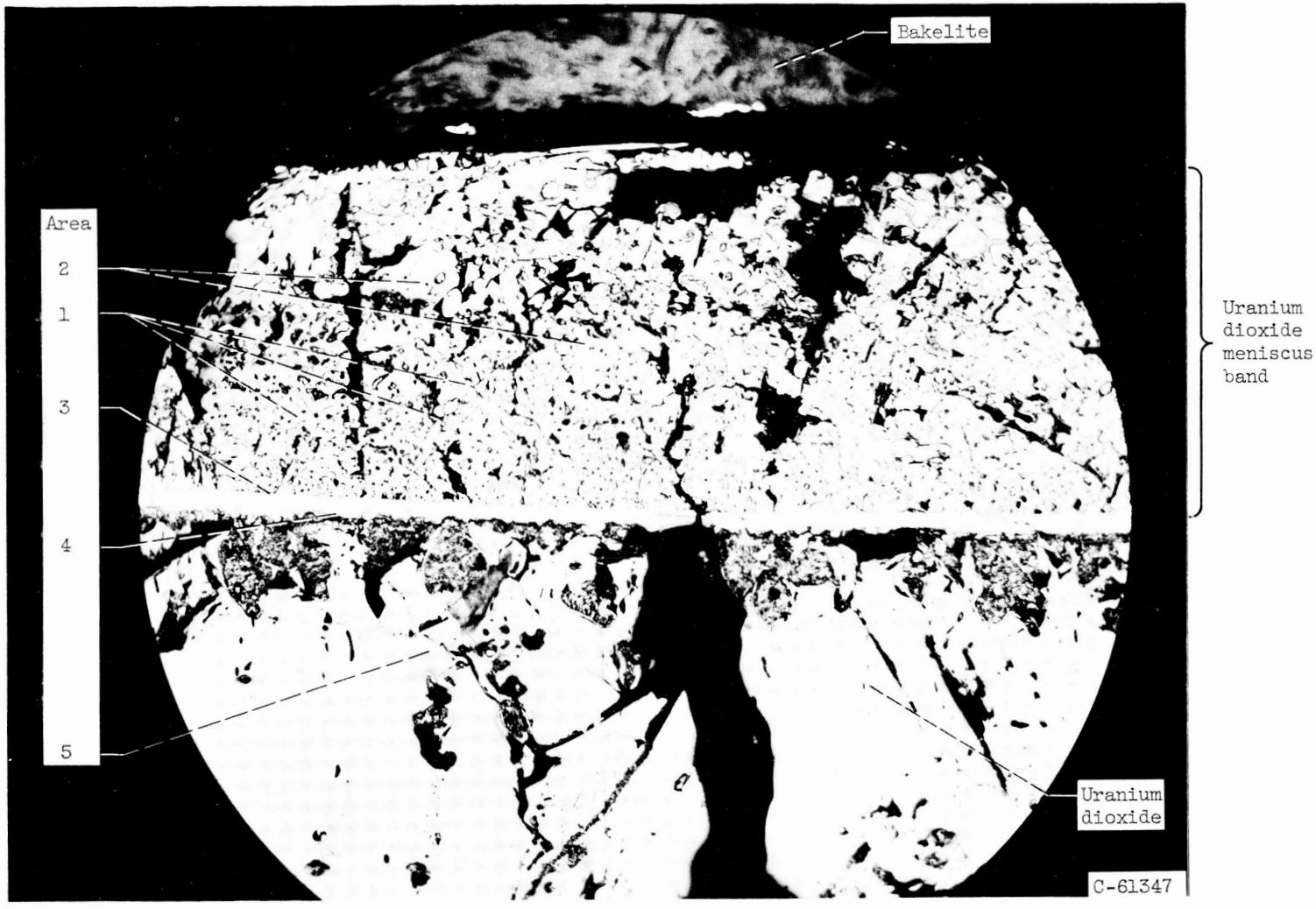

(a) Short-test-time crucible.

Figure 9. - Photomicrograph of cross section of uranium dioxide meniscus region in hafnium carbide crucible; etchant, nitric acid plus hydrofluoric acid; ×250.

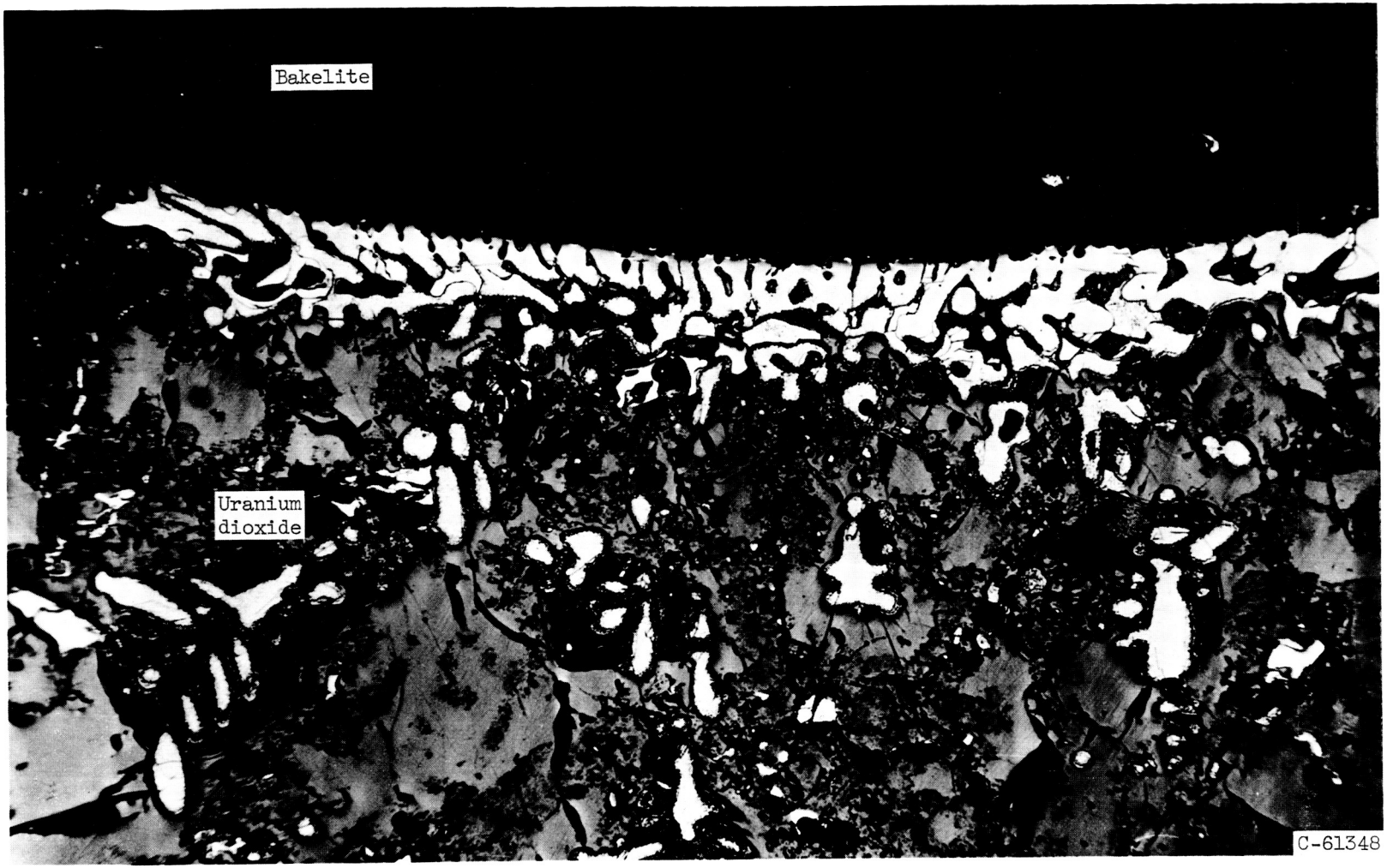

(b) Full-test-time crucible.

Figure 9. - Concluded. Photomicrograph of cross section of uranium dioxide meniscus region in hafnium carbide crucible; etchant, nitric acid plus hydrofluoric acid; ×250.

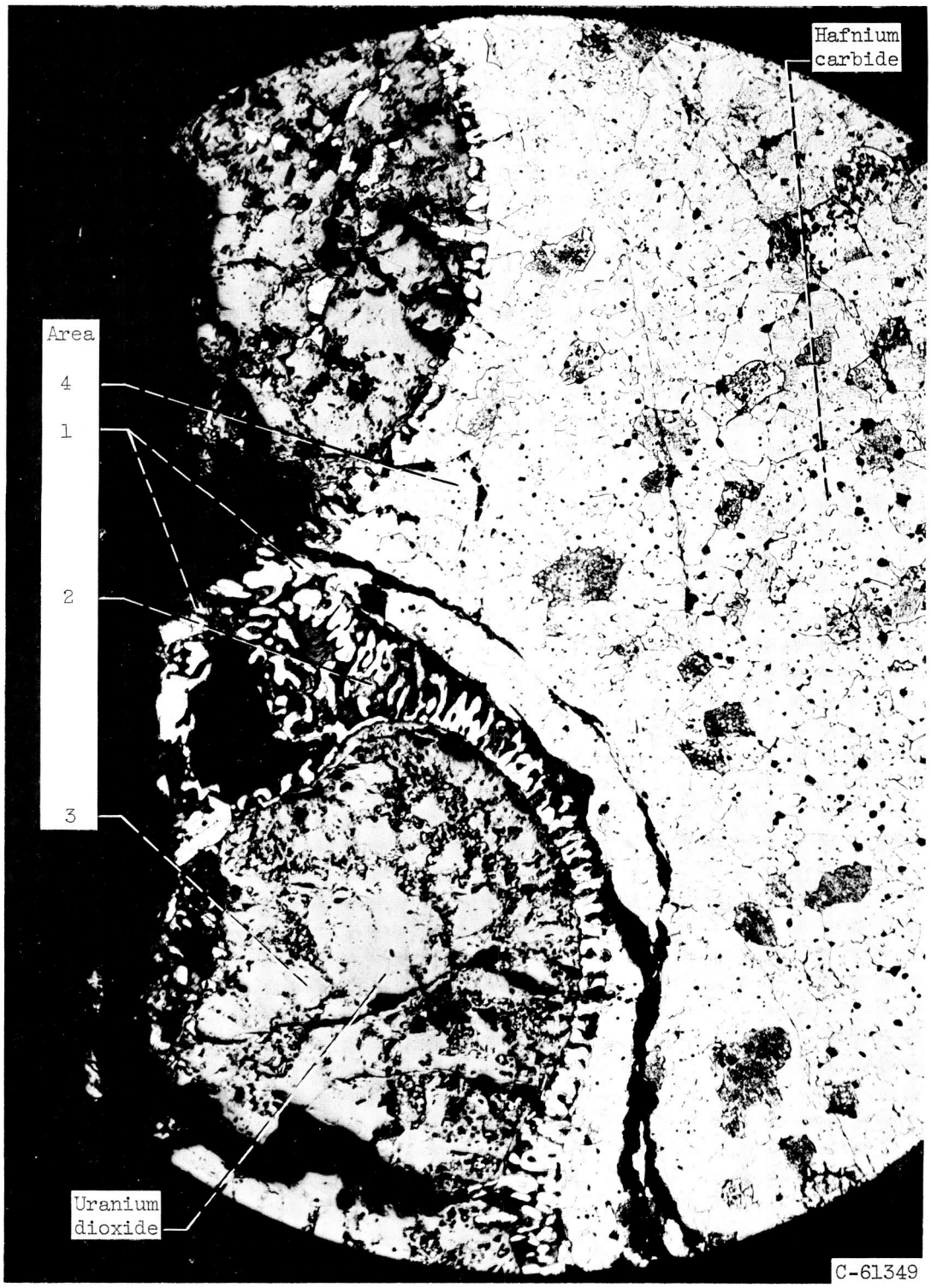

Figure 10. - Photomicrograph of cross section of full-test-time hafnium carbide crucible at thread apex region; etchant, nitric acid plus hydrofluoric acid; ×100.